JOURNAL OF AIRCRAFT
Vol. 45, No. 2, March–April 2008

Engineering Notes

ENGINEERING NOTES are short manuscripts describing new developments or important results of a preliminary nature. These Notes should not exceed 2500 words (where a figure or table counts as 200 words). Following informal review by the Editors, they may be published within a few months of the date of receipt. Style requirements are the same as for regular contributions (see inside back cover).

Engine Speed and Velocity Controller Development for Small Unmanned Aerial Vehicles

Fei-Bin Hsiao,* Sheng-Yen Hsieh,† Woei-Leong Chan,‡ and Ying-Chih Lai‡
National Cheng Kung University, Tainan 70101, Taiwan, Republic of China

DOI: 10.2514/1.33709

Nomenclature

C_{PI}	=	proportional–integral controller
K_i	=	I-control gain
K_p	=	P-control gain
N_{rpm}	=	engine speed in the frequency domain, rpm
n_{rpm}	=	engine speed, rpm
T	=	thrust
U	=	velocity along the X_B axis of the aircraft in the frequency domain
u	=	velocity along the X_B axis of the aircraft
V	=	freestream velocity
Δ_e	=	elevator deflection in the frequency domain
Δ_{th}	=	throttle area in the frequency domain
δ_e	=	elevator deflection angle
δ_{th}	=	throttle area

I. Introduction

VELOCITY control is an essential element of an autopilot in different phases of flight. To achieve better flight quality, the Remotely Piloted Vehicle and Micro-Satellite Research Laboratory (RMRL) decided to design a velocity controller for the SWAN (surveillance, watch, autonomous, navigation) unmanned aerial vehicle (UAV) (Fig. 1) [1–3]. Nonlinear and linear models of the engine were derived to accomplish the task and, based on the linear model, the velocity controller was designed. Simulation using the nonlinear model was performed before the controller was implemented on the SWAN UAV.

Received 26 July 2007; accepted for publication 23 November 2007.

*Professor, Institute of Aeronautics and Astronautics, 1 University Road; fbhsiao@mail.ncku.edu.tw. Fellow AIAA.
†M.S. Student, Institute of Aeronautics and Astronautics, 1 University Road.
‡Ph.D. Student, Institute of Aeronautics and Astronautics, 1 University Road.

II. Identification and Characteristics of Engine Models

A. Identification of the Nonlinear Engine Model

The SWAN UAV uses the O.S. Engines FS-120 Surpass III four-stroke nitro engine with an APC 17 × 6 propeller. Several tests were conducted in a wind tunnel to model the relation between throttle area and engine speed in steady state at sea-level temperature and air density, which results in

$$\begin{aligned} n_{\mathrm{rpm}} = {} & 2.474 \times 10^{-6} V^3 \delta_{\mathrm{th}}^3 - 1.034 \times 10^{-4} V^2 \delta_{\mathrm{th}}^3 + 6.200 \\ & \times 10^{-4} V \delta_{\mathrm{th}}^3 + 0.01228 \delta_{\mathrm{th}}^3 - 4.346 \times 10^{-4} V^3 \delta_{\mathrm{th}}^2 \\ & + 0.01782 V^2 \delta_{\mathrm{th}}^2 - 0.09154 V \delta_{\mathrm{th}}^2 - 3.002 \delta_{\mathrm{th}}^2 + 0.02041 V^3 \delta_{\mathrm{th}} \\ & - 0.8054 V^2 \delta_{\mathrm{th}} + 2.607 V \delta_{\mathrm{th}} + 242.5 \delta_{\mathrm{th}} - 0.2478 V^3 \\ & + 12.92 V^2 - 63.34 V + 1215 \end{aligned} \tag{1}$$

The engine is a first-order system with a transportation delay of 0.5 s. Because the sampling rate was 10 Hz, the discrete-time transfer function of the transient response was derived as Eq. (2). It indicates that the transient response takes 1.75 s to reach 95% of the steady-state response.

$$\frac{\Delta_{\mathrm{th,delayed}}(z)}{\Delta_{\mathrm{th}}(z)} = \frac{0.1573}{z - 0.8427} \tag{2}$$

Wind-tunnel tests were also conducted to model the relationship between engine speed and thrust under different freestream velocities, which takes the form

$$\begin{aligned} T = {} & -2.361 \times 10^{-9} V^2 n_{\mathrm{rpm}}^2 + 5.086 \times 10^{-8} V n_{\mathrm{rpm}}^2 + 5.454 \\ & \times 10^{-7} n_{\mathrm{rpm}}^2 + 3.102 \times 10^{-5} V^2 n_{\mathrm{rpm}} - 6.855 \times 10^{-4} V n_{\mathrm{rpm}} \\ & + 0.002452 n_{\mathrm{rpm}} - 0.1380 V^2 + 1.743 V - 7.392 \end{aligned} \tag{3}$$

B. Identification of the Linear Engine Model

Using Eq. (1), the linear model can be obtained by performing partial differentiation of the equation against throttle area and then substituting the partial derivatives into Eq. (4).

$$\Delta n_{\mathrm{rpm}}(t) = \frac{\partial n_{\mathrm{rpm}}(t)}{\partial \delta_{\mathrm{th}}(t)} \Delta \delta_{\mathrm{th}}(t) \tag{4}$$

From flight data under cruise conditions in which the average freestream velocity $V = 22.22$ m/s and the throttle area $\delta_{\mathrm{th}} = 57\%$, the partial derivatives were calculated as

$$\frac{\partial n_{\mathrm{rpm}}(t)}{\partial \delta_{\mathrm{th}}(t)} = 32.77 \text{ rpm}/\% \tag{5}$$

Using Eq. (2) and introducing a transport delay of 0.5 s, the discrete-time linear model of throttle area to engine speed was obtained. They are as presented in Eq. (6), with a sampling rate of 0.1 s.

$$\frac{N_{\mathrm{rpm}}(z)}{\Delta_{\mathrm{th}}(z)} = \frac{5.155}{z^5(z - 0.8187)} \tag{6}$$

Fig. 1 SWAN UAV.

Comparing the simulation of Eq. (6) with the real flight data, as shown in Fig. 2a, the derived linear model simulation fits considerably well. The disparities are mainly caused by noise and the effects of elevator deflection.

Similarly, the linear model of engine speed to thrust is presented in Eq. (7). Also, under cruise conditions in which the average freestream velocity $V = 22.22$ m/s and the throttle area $\delta_{\text{th}} = 57\%$, from Eq. (1), $n_{\text{rpm}} = 7812.3$ rpm. Using Eq. (5), the partial derivatives were calculated and are presented as Eq. (8).

$$\Delta T(t) = \frac{\partial T(t)}{\partial n_{\text{rpm}}(t)} \Delta n_{\text{rpm}}(t) \tag{7}$$

$$\frac{\partial T(t)}{\partial n_{\text{rpm}}(t)} = 0.0105 \text{ N/rpm} \tag{8}$$

It was assumed that the transient state of engine speed to thrust relation is negligible. Aided by the method mentioned in [4], the discrete-time transfer function of thrust to velocity was derived as Eq. (9). Using Eq. (8), the discrete-time transfer function of engine speed to velocity is presented in Eq. (10), with a sampling rate of 0.1 s.

$$\frac{U(z)}{T(z)} = \frac{0.008984z^3 - 0.01299z^2 + 0.005222z - 0.001222}{z^4 - 2.435z^3 + 2.013z^2 - 0.7116z + 0.1347} \tag{9}$$

$$\frac{U(z)}{N_{\text{rpm}}(z)} = \frac{9.434 \times 10^{-5} z^3 - 0.0001363z^2 + 5.484 \times 10^{-5} z - 1.283 \times 10^{-5}}{z^4 - 2.435z^3 + 2.013z^2 - 0.7116z + 0.1347} \tag{10}$$

It was assumed that $u(t) \approx V(t)$. Only the throttle command was given during the validation process. Figure 2b shows the comparison of responses of freestream velocity due to engine speed variation. The simulation result fits the trend of variation, but the magnitude is somewhat different. Because many factors contribute to the change of velocity, the assumption of $u(t) \approx V(t)$ is only true if the angle of attack and angle of sideslip were both very small. Thus, the linear model was considered to be acceptable.

III. Velocity Controller of SWAN

A. Concepts of Velocity Control

The velocity controller block diagram is shown in Fig. 3. The outer loop calculates differences between the desired airspeed and the current airspeed and determines the desired engine speed. The inner loop calculates the difference between the desired engine speed and the current engine speed. Then the controller calculates the desired throttle.

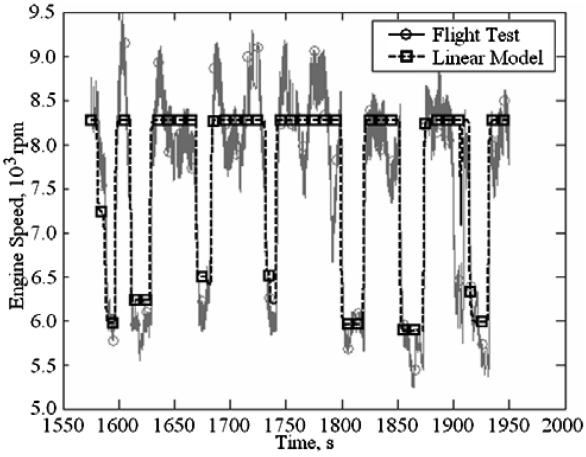

a) Engine speed versus time

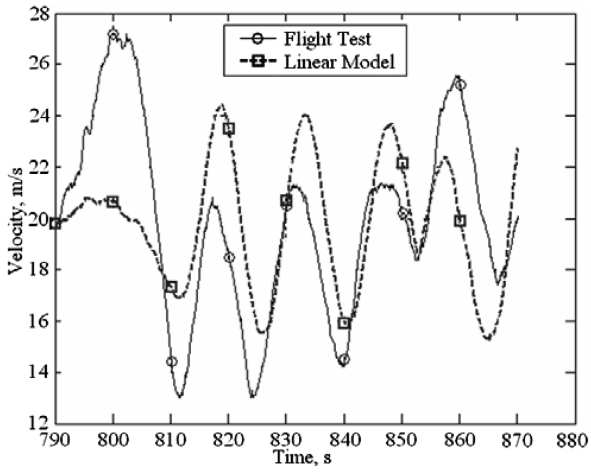

b) Velocity versus time

Fig. 2 Comparison of flight data and single-input/single-output linear model simulation.

B. Inner Loop

The inner loop is a feedback control that uses throttle to control engine speed. Step-response analysis by using P-control found that a steady-state error is unavoidable. Thus, proportional–integral (PI) control was used. D-control was not used, due to the noisy tachometer feedback. The resultant controller is presented as Eq. (11). K_p and K_i are assigned to be 0.01676%/rpm and 0.0284%/(rpm · s), respectively.

$$C_{\text{PI}}(z) = \frac{0.01676z - 0.01392}{z - 1} \tag{11}$$

C. Outer Loop

The outer loop is a feedback control that uses engine speed to control velocity. Similar to the inner loop, steady-state error is unavoidable with P-control; thus, PI control was used. D-control was not used, due to the noisy airspeed sensor feedback. The resultant controller is presented as Eq. (12). K_p and K_i are assigned to be 787.5 rpm/(m/s) and 315 rpm/m, respectively.

$$C_{\text{PI}}(z) = \frac{787.5z - 756}{z - 1} \tag{12}$$

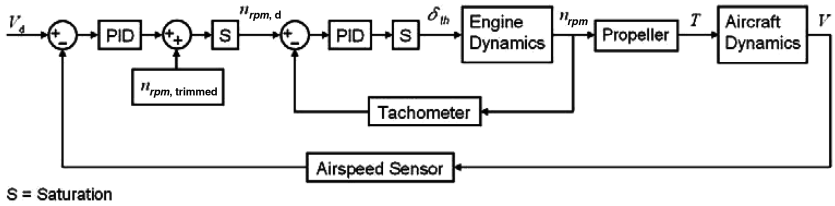

Fig. 3 Velocity controller.

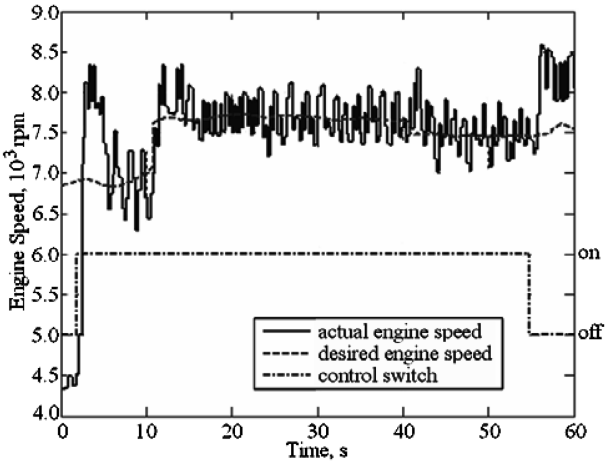

Fig. 4 Result of inner-loop control.

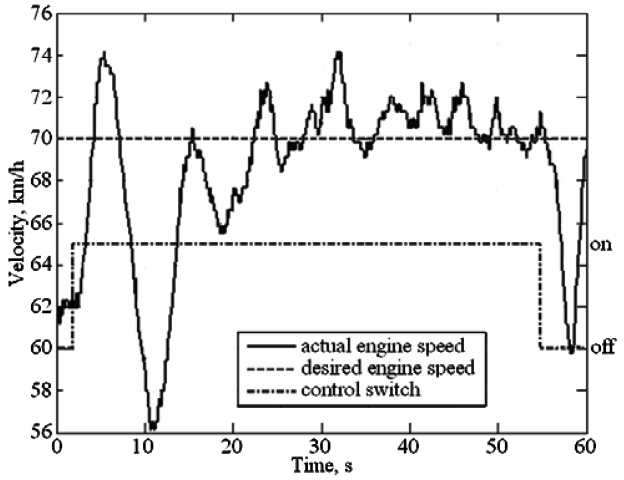

Fig. 5 Result of outer-loop control.

IV. Flight Test Validation

The velocity controller was validated through flight tests. Velocity control, altitude control, and heading control were engaged. The desired values of altitude, heading, and velocity were 250 m, 180° (south), and 70 km/h, respectively. The results are shown in Figs. 4 and 5. The flight data show that the aircraft was lower than the desired altitude initially; thus, the aircraft was climbing right after the control systems were engaged, which resulted in the decrease of velocity. Therefore, the velocity controller increased the desired engine speed to gain more thrust. During the steady state, the velocity controller was capable of maintaining the velocity within a 3-km/h error.

V. Conclusions

A nonlinear engine model was obtained through a series of engine tests in a wind tunnel. The nonlinear model was used in simulation before flight test validation. The simulation result is not presented. A linear engine model was obtained by performing linearization on the nonlinear model. The linear model was validated by comparing the linear model simulation result with flight data. The linear model was used in the controller design. A two-loop feedback velocity controller using a proportional–integral–differential control method was designed and implemented on the SWAN UAV. It was successfully validated in flight tests with a steady-state error of 3 km/h.

Acknowledgments

This research was supported by the National Science Council and National Cheng Kung University, contracts NSC 95-2221-E-006-255 and D95-3300. The authors thank Richard Hirst of JPBH Consulting Limited for his advice during the preparation of the manuscript.

References

[1] Hsiao, F. B., Chien, Y. H., Liu, T. L., Lee, M. T., Chang, W. Y., Han, S. Y., and Wang, Y. H., "A Novel Unmanned Aerial Vehicle System with Autonomous Flight and Auto-Lockup Capability," AIAA Paper 2005-1050, Jan. 2005.

[2] Hsiao, F. B., Lai, Y. C., Tenn, H. K., Hsieh, S. Y., Chen, C. C., Chan, W. L., and Hirst, R., "The Development of an Unmanned Aerial Vehicle System with Surveillance, Watch, Autonomous Flight & Navigation Capability," *21st International Unmanned Air Vehicle Systems Conference*, Univ. of Bristol, Bristol, England, U.K., Apr. 2006, pp. 9.1–9.12.

[3] Hsiao, F. B., Lee, M. T., Chien, Y. H., Chang, W. Y., Liu, T. L., and Payne, Y. J., "The Development of a Low Cost Autonomous Surveillance UAV System," *Transactions of The Aeronautical and Astronautical Society of the Republic of China*, Vol. 35, No. 4, Dec. 2003, pp. 307–316.

[4] Roskam, J., *Airplane Design, Part 6: Preliminary Calculation of Aerodynamic, Thrust and Power Characteristics*, Roskam Aviation and Engineering Corp., Ottawa, KS, 1990, pp. 371–461.